

Exploring the immune landscape of cirrhosis through Weighted Gene Co-expression Network Analysis

Basang Zhuoma¹, Ci Yang¹, Wenhai Wang², Yibi Ranhen^{1*}¹ Department of Gastroenterology, Lhasa People's Hospital, Lhasa, China² Department of Gastroenterology, Beijing Friendship Hospital, Capital Medical University, Beijing, China

ARTICLE INFO

Original paper

Article history:

Received: March 09, 2023

Accepted: June 13, 2023

Published: June 30, 2023

Keywords:

metagenomic next-generation sequencing, microbial culture, pathogen, diagnosis

ABSTRACT

Cirrhosis is a persistent hepatic ailment that emerges from a range of causes, including viral infections, alcoholic liver disease, and non-alcoholic fatty liver disease. It is distinguished by the replacement of normal liver parenchyma with fibrous scar tissue, culminating in the development of hepatic insufficiency, portal hypertension, and eventual liver collapse. Several molecular and cellular mechanisms contribute to cirrhosis' pathogenesis, including activation of immune cells and dysregulation of immune-related pathways. Weighted Gene Co-expression Network Analysis (WGCNA) is a powerful data mining application used to identify gene modules and hub genes that are closely associated with specific phenotypes or conditions of interest. In this study, we performed WGCNA on publicly available gene expression datasets and subsequently assessed the roles of immune-related genes in the etiology and progression of cirrhosis, intending to explore potential therapeutic targets for this disease. GSE36411 gene expression profiling was extracted from the Gene Expression Omnibus repository (GEO). The transcriptomic data were submitted to Weighted Gene Co-expression Network Analysis (WGCNA) to screen for the presence of key genes, and immune-related genes were filtered by comparison to the InateDB database. Cancer Genome Atlas (TCGA) was included in the study to validate the significant modules generated from WGCNA. The key gene interaction network was constructed using GeneMANIA and Metascape. Kaplan-Meier method and Spearman correlation were used to evaluate the correlation of immune-related genes with prognosis, tumor microenvironment, and immune cell infiltration. Finally, we explored a possible mechanism using gene set enrichment (GSEA) analyses. In total, 2,102 differentially expressed genes (DEGs) were identified from the gene expression profile dataset. A weighted gene co-expression network analysis was performed, resulting in the classification of genes into 3 modules. Among these modules, the turquoise module was found to be most closely associated with cirrhosis. By comparing the turquoise module genes with an InateDB immune-related gene set, we identified 157 immune-associated genes. In addition, our study found that many hub genes are strongly associated with the number of immune-related genes in liver cirrhosis, in addition to a few modules associated with immune infiltration. It turns out that these hub genes were engaged in migration, activation, and immune cell regulation, as well as in the signaling pathways that drive the immune response to infection. Our research offered a deeper understanding of the underlying processes of immune infiltration in cirrhosis and also suggested potential treatment options for this troublesome condition. Our results demonstrate the effectiveness of WGCNA in uncovering new knowledge regarding the biology of cirrhosis and the function of the immune system in this disease. More studies ought to focus on the validation of the identified hub genes and the determination of their clinical relevance. These results could serve as the basis for the creation of more potent therapies for those with liver cancer linked to cirrhosis.

Doi: <http://dx.doi.org/10.14715/cmb/2023.69.6.25>Copyright: © 2023 by the C.M.B. Association. All rights reserved. 

Introduction

Cirrhosis is a chronic hepatic disorder characterized by progressive and irreversible fibrosis of the liver tissue, which leads to significant morbidity and mortality (1). This disease is marked by the accumulation of scar tissue in the liver, resulting in the development of nodules and fibrosis. Over time, this can cause liver dysfunction and may also elevate the risk of liver cancer (2).

The immune system is crucial in the onset and progression of cirrhosis. In response to liver injury during the early stages of the disease, the immune system initiates inflammatory pathways, which can aid in the clearance of

damaged cells and facilitate tissue repair (3). However, if the injury persists, the ongoing immune response can contribute to the development of fibrosis and the formation of nodules (4). The hepatic stellate cell (HSC) is a crucial cell type in the progression of cirrhosis (5). HSCs can communicate with immune cells such as Kupffer cells and T cells, leading to the activation of inflammatory pathways. Additionally, other immune cells like natural killer cells, neutrophils, and macrophages are also involved in the pathogenesis of cirrhosis (6-8). These cells can generate cytokines and chemokines that possess pro-inflammatory properties, which can exacerbate HSC activation and encourage the onset of fibrosis (9).

* Corresponding author. Email: yibiranhen@sina.com

However, liver cirrhosis has a highly variable prognosis, which is influenced by variables such as disease etiology, severity, complications, and comorbidities. It is estimated that the lifespan of a patient with advanced cirrhosis is reduced to one or two years.

The transcriptomics method has recently emerged as a powerful tool for studying complex diseases like cirrhosis. Large-scale gene expression datasets may be used to identify groupings or modules of co-expressed genes using the computational method known as weighted gene co-expression network analysis (WGCNA) (10). It has been widely used in biological research for identifying new therapeutic targets and biomarkers for disease diagnosis and prognosis (11, 12).

In the current investigation, we employed WGCNA to scrutinize the transcriptomic data of cirrhosis, to pinpoint particular modules that are closely linked to immune infiltration, as well as identifying their corresponding hub genes. Our findings shed new light on the underlying processes of immune infiltration in cirrhosis and suggest future therapeutic targets for this complicated illness.

Materials and Methods

Data source

Figure 1 illustrates the workflow followed in this study. The mRNA expression profile microarray GSE36411, which was submitted by Wang *et al.* (13), was obtained from the GEO database. This dataset comprises mRNA expression profiles of human hepatocellular carcinoma (HCC) tissue samples from both tumor and non-tumor groups. The non-tumor group has two subgroups: a normal liver group (NL, $n = 20$) and a liver cirrhosis group (LC, $n = 20$). In this study, we utilized the NL and LC group of GSE36411 to construct co-expression networks and identify hub genes associated with cirrhosis. The dataset was sequenced by the GPL10558 platform (Illumina HumanHT-12 V4.0 expression beadchip). The dataset was normalized by applying the quantile normalization method in the linear models for microarray data, followed by \log_2 transformation, as indicated in the data processing information of GSE36411.

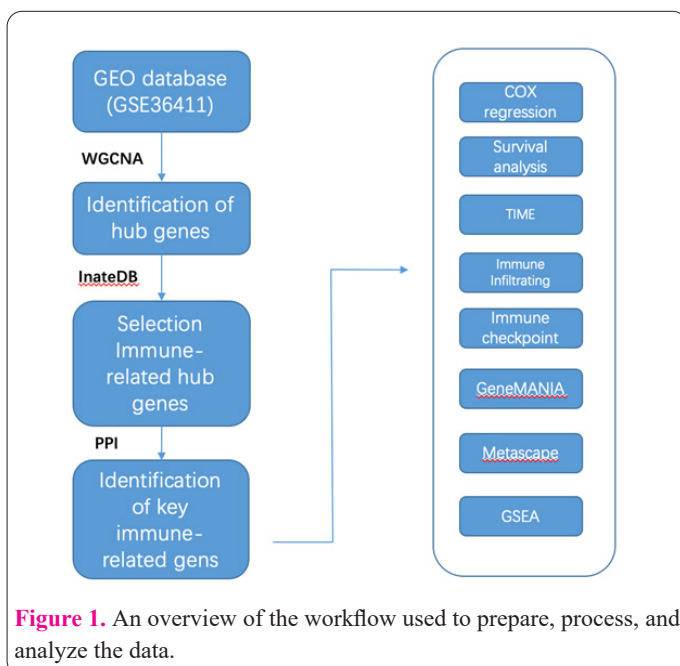


Figure 1. An overview of the workflow used to prepare, process, and analyze the data.

DEGs identification and WGCNA

After identifying the differentially expressed genes (DEGs) using *deseq2*, we used the weighted gene co-expression network analysis (WGCNA) to build a gene co-expression network. We used a gradient approach to test for scale independence and mean connectedness, with power values ranging from 1 to 20, and we were able to produce a scale-free network with a degree of independence greater than 0.80 (10). After transforming the adjacency matrix into a topological overlap matrix (TOM), a hierarchical average linkage clustering analysis was executed on the gene dendrogram. This approach facilitated gene clustering into distinct gene modules according to the TOM-based dissimilarity measure.

Hub genes identification and Protein-Protein Interaction network

Those genes with kME (eigengene-based connectivity) values in the top 30% of genes were considered hub genes for the module-trait correlation analysis. Using the InateDB database, we selected immune-related genes and analyzed their protein-protein network interactions (PPI) with help of the Search Tool for Retrieval Interacting Genes (STRING) database. Based on the ranking of PPI-connected nodes from most to least, we selected the top 10 hub genes belonging to immune genes as key immune genes.

Differential expression analysis

The dataset of 33 different types of cancer collected from TCGA was analyzed using the DESeq2 package (1.34.0) for pairwise differential expression analysis, which produced DEGs (or transcripts) between cancer and non-neoplastic control tissue. P adjusted value < 0.05 and \log_2 fold change (FC) ≥ 1 were chosen as the cut-off criteria.

Kaplan-Meier curve

The R ‘Survival’ and ‘Survminer’ packages facilitate survival analysis and visualization. Cox regression analysis was conducted to identify independent risk factors associated with LC.

Construction of Co-Expression Network

The similarity expression patterns of differentially expressed genes (DEGs) of the GSE36411 microarray dataset were constructed using the R package ‘WGCNA’ (10). The WGCNA package was used to analyze all DEGs and determine the optimal soft thresholding power. Subsequently, the DEGs were grouped into different modules based on their weighted co-expression network and assigned color labels. The correlation between each module and LC or control groups was investigated. The module that displayed the highest correlation with LC was considered a key module for further enrichment analysis.

Gene Ontology and pathway enrichment analysis

KEGG pathway analysis and Gene Ontology (GO) analysis (which includes biological process, cellular component, and molecular function) were both carried out in the major module created by WGCNA. To further visualize the function and route words in the R program, the terms were obtained.

Tumor Immune Microenvironment and Infiltrating Analysis

To estimate the number of immune cells present in tumor samples, a method called 'Estimation of STromal and Immune cells in MAlignant Tumours using Expression data' (ESTIMATE1.0) was applied. To obtain a more precise estimation of immune cell infiltrating levels, we utilized the TIMER2.0 tool, which is tailored specifically for The Cancer Genome Atlas (TCGA) data, in our investigation. Additionally, the xCell algorithm (<https://xcell.ucsf.edu/>) was employed to quantify immune cell numbers and analyze cell type enrichment.

GeneMANIA and signaling pathways analysis

GeneMANIA (<http://www.genemania.org>) is an online protein-protein interaction network database that provides a user-friendly platform to explore functional connections and interactions between genes. GeneMANIA was used to construct a core gene network to explore possible mechanisms in patients with OA in this study. The genes identified in the network were subjected to gene ontology (GO) analysis using the Metascape tool (<https://metascape.org/gp/index.html#/main/step1> v3.5, San Diego, CA, USA).

Gene Set Enrichment Analysis

To assess the degree of enrichment of the KEGG pathway in patients with LC, Gene Set Enrichment Analysis (GSEA4.3) was employed. The GSEA desk application's transcriptome data were imported strictly following the website's instructions. The criterion for the significant gene sets was taken to be P-value < 0.05 and FDR < 0.25.

Statistical analysis

To investigate the statistical significance of the differences among groups, a nonparametric test or t-test was used, depending on the parameters of the data distribution. The program R3.5.3 was used in our study, and statistical significance was defined when P-value < 0.05.

Results

WGCNA identifies hub genes from key modules

A total of 2,441 DEGs were identified for further analysis. Using the WGCNA analysis, 19 co-expression modules were constructed (Figure 2A). A correlation analysis between modules and traits revealed that the module in blue had the greatest association with clinical characteristics (cor =0.57, P=6.2e-102) (Figure 2B, C). As a result, the blue module was chosen for further examination. We applied to GO and KEGG analysis to determine the likely biological roles that the genes in the blue module may play. According to biological process GO analysis, the blue module's genes were mostly engaged in T cell activation and cell adhesion (Figure 2D). As a result, we selected 157 immune-related genes as immune-related hub genes by comparing all the DEGs in the blue module with the InateDB database. Furthermore, we selected the 30% of genes that appeared at the top of the kME rank. The higher the intramodular connectivity (kME) value of a gene, the more representative its expression within a module is. And String was used to create a protein-protein interaction (PPI) network using these genes (Figure 2E). The 10 genes with the highest degree of correlation were selected as immune-related hub genes, including CCL5, CXCR4,

CCR7, FCGR2A, IL7R, SYK, CD27, SPP1, IFI16, and MMP7.

Hub genes interaction network and enrichment analysis

We used the "GeneMania" application to create a gene-gene interaction network of the 10 immune-related hub genes to highlight their probable biological activities (Figure 3A). The most highly correlated genes with other genes were CCL5, CXCR4, CCR7, IL7R, and CD27. The hub genes were mostly implicated in the inflammatory response, control of the defensive response, and negative regulation of the immune response, according to further functional enrichment analysis performed using the Metascape program (Figure 3B).

Validation of the hub genes

To further examine the prognostic significance of hub genes as shared indicators, we performed Cox regression analysis on 33 separate cancer types from the TCGA dataset. 153 genes met the criteria ($|HR| > 1$ and $p < 0.05$). Based on gene expression levels, we categorized each can-

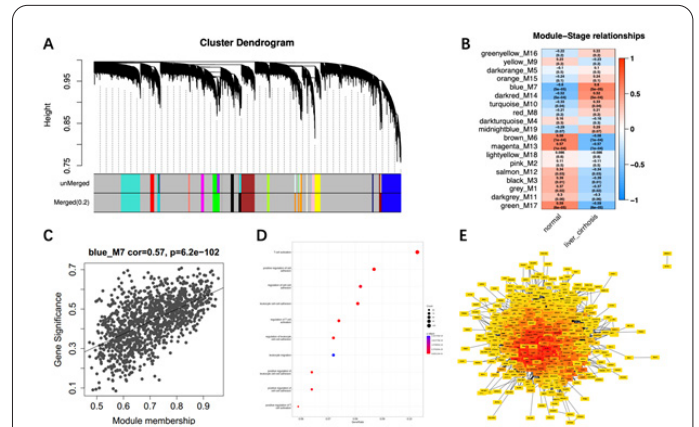


Figure 2. Identification of the key module and immune-related genes associated with liver cirrhosis. (A) Cluster dendrogram of differentially expressed genes related to liver cirrhosis. (B) Heatmap of the module-trait connection. Module eigengenes that list the modules discovered during the clustering study are clustered hierarchically. The column denotes the characteristic, whereas the row denotes the module. P-values are indicated within boxes. (C) Scatterplot of Gene significance versus module membership in the blue module. (D) Dot plot of GO analysis for all genes in the blue module of cluster dendrogram. (E) Map of protein-protein interactions of the hub genes. The warmer the color, the closer the gene interacts with other genes.

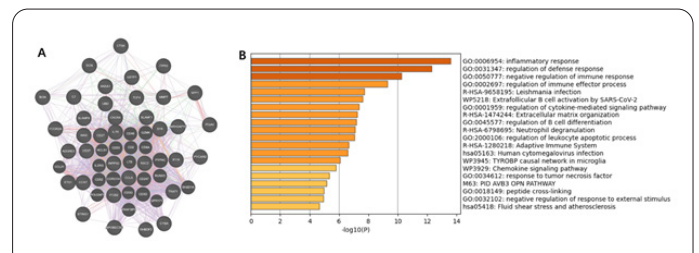


Figure 3. (A) Gene-gene interaction network of hub genes. The degree of interactions is represented by the node size. The types of gene-gene interactions are represented by the inter-node connection lines, while the network types are represented by the line colors. (B) Histogram of functional enrichment analysis of key hub genes. The enriched terms are colored by p-value, and distinct colors indicate enriched pathways.

cer type into a high-expression group and a low-expression group. The overall survival (OS) of these 153 genes was calculated (Figure 4). As a consequence, 119 genes were shown to be strongly linked with disease prognosis ($P < 0.05$). Particularly, the association between the hub genes and overall survival status in TCGA datasets was shown in Figure 4. High CCL5 expression levels were correlated with a worse OS in thymoma (THYM). As for that, CXCR4 was positively related to poor OS in stomach adenocarcinoma (STAD). While OS was significantly reduced in patients with elevated expression of CCR7, IL7R, and CD27 in sarcoma (SARC), lung adenocarcinoma (LUAD), and head and neck squamous cell carcinoma (HNSC) ($P \leq 0.001$).

Immune infiltration and tumor microenvironment analysis

To gain further insight into how hub genes regulate immune responses in the tumor microenvironment (TME), we investigated TME immune backgrounds in 33 different cancer types in TCGA using TIMER, xCell, and ESTIMATE. First, we used ESTIMATE to provide information on the amount of stromal and immune cells in gene expression tumor samples (14). A Spearman correlation study was run across hub genes and ESTIMATEScore, ImmuneScore, as well as StromalScore. Our results revealed a significant correlation between selected genes and ESTIMATE parameters with P values < 0.05 . Additionally, to provide a more robust estimation of immune infiltration levels, we used TIMER and applied xCell algorithms for immune cell quantification and cell type enrichment analysis (15, 16). CCL5 was found to be strongly associated with CD8+T cells in STAD (R-value = 0.82, $P = 2.2e-16$), bile duct cancer (CHOL (R-value = 0.79, $P = 4.19E-07$), and cervical squamous cell carcinoma (CSC) and endocervical adenocarcinoma (CESC) (R-value = 0.77, $P < 2.2e-16$). CXCR4 expression was strongly associated with CD4 + T cells and dendritic cells in THYM (R-value = 0.85, $P < 2.2e-16$; Rvalue = 0.84, $P < 2.2e-16$) and CHOL (R-value = 0.78, $p = 4.14E-07$; R-value = 0.84, $P = 2.49E-07$). Macrophages (R-value = 0.77, $P = 5.78E-07$) and B cells (R-value = 0.76, $P = 8.09E-07$) were also strongly correlated in CHOL. Breast cancer cell line CCR7 was significantly associated with a wide range of cells such as B cells, CD4+T cells, CD8+T cells, and neutrophils. (R-value = 0.51, $P < 2.2e-16$; R-value = 0.72, $P < 2.2e-16$; R-value = 0.55, $P < 2.2e-16$; R-value = 0.67, $P < 2.2e-16$) and CESC (R-value = 0.62, $P < 2.2e-16$; R-value = 0.59, $P < 2.2e-16$; R-value = 0.51, $P < 2.2e-16$; R-value = 0.60, $P < 2.2e-16$). Strong correlation was found between IL7R and dendritic cells in thyroid carcinoma (THCA) (R-value = 0.85, $P < 2.2e-16$) and CHOL (R-value = 0.85, $P = 7.74E-08$), as well as with CD4+T cells in CHOL (R-value = 0.82, $P = 1.88E-07$) and THYM (R-value = 0.81, $P < 2.2e-16$). CD27 was highly relevant to CD8+T cells in head and neck squamous cell carcinoma (HNSC) (R-value = 0.77, $P < 2.2e-16$), CHOL (R-value = 0.76, $P = 6.75E-07$), adrenocortical carcinoma (ACC) (R-value = 0.75, $P < 2.2e-16$), kidney renal clear cell carcinoma (KIRC) (R-value = 0.67, $P < 2.2e-16$), and ovarian serous cystadenocarcinoma (OV) (R-value = 0.66, $P < 2.2e-16$). The results showed that hub genes were significantly associated with the tumor microenvironment (TIM) and immune cells.

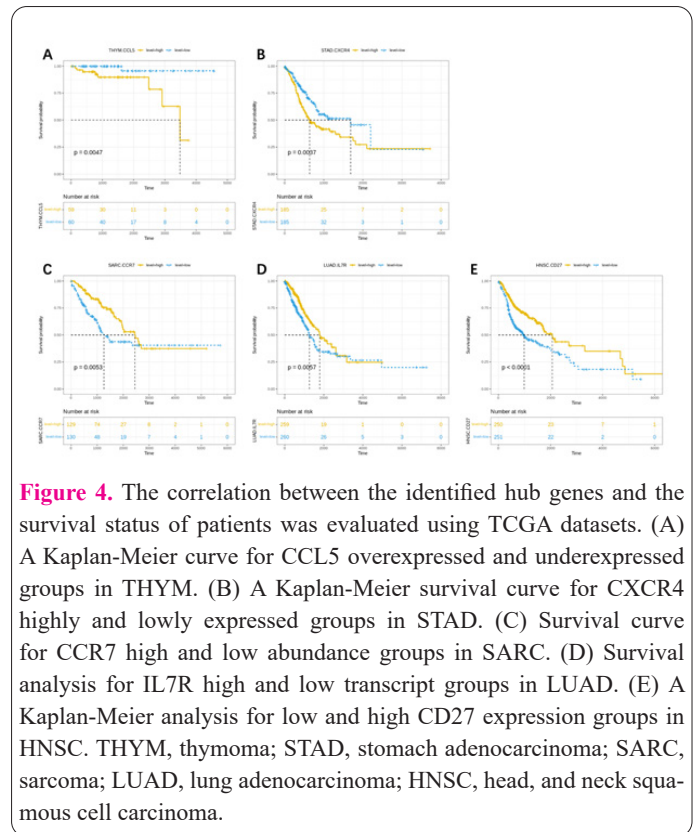


Figure 4. The correlation between the identified hub genes and the survival status of patients was evaluated using TCGA datasets. (A) A Kaplan-Meier curve for CCL5 overexpressed and underexpressed groups in THYM. (B) A Kaplan-Meier survival curve for CXCR4 highly and lowly expressed groups in STAD. (C) Survival curve for CCR7 high and low abundance groups in SARC. (D) Survival analysis for IL7R high and low transcript groups in LUAD. (E) A Kaplan-Meier analysis for low and high CD27 expression groups in HNSC. THYM, thymoma; STAD, stomach adenocarcinoma; SARC, sarcoma; LUAD, lung adenocarcinoma; HNSC, head, and neck squamous cell carcinoma.

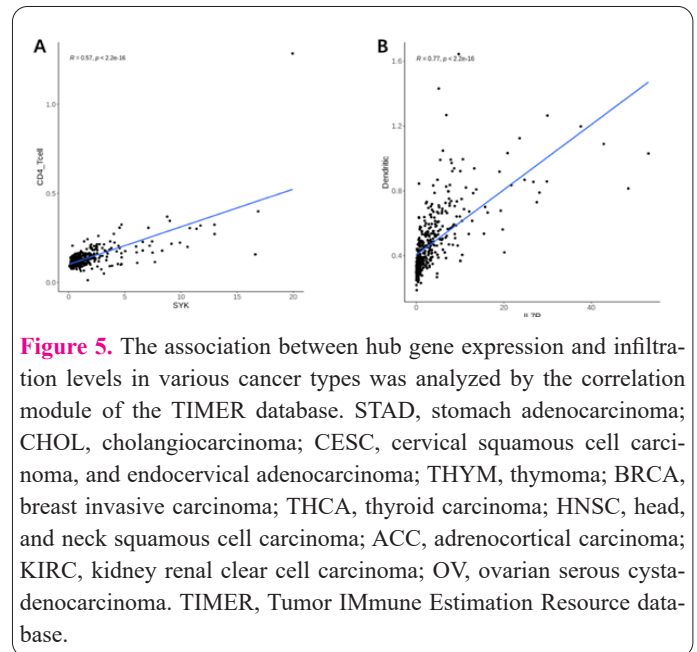


Figure 5. The association between hub gene expression and infiltration levels in various cancer types was analyzed by the correlation module of the TIMER database. STAD, stomach adenocarcinoma; CHOL, cholangiocarcinoma; CESC, cervical squamous cell carcinoma, and endocervical adenocarcinoma; THYM, thymoma; BRCA, breast invasive carcinoma; THCA, thyroid carcinoma; HNSC, head, and neck squamous cell carcinoma; ACC, adrenocortical carcinoma; KIRC, kidney renal clear cell carcinoma; OV, ovarian serous cystadenocarcinoma. TIMER, Tumor IMMune Estimation Resource database.

Immune checkpoint analysis

Immune cell infiltration in tumors is directly associated with clinical outcomes, leading to the development of multiple treatment modalities such as chemotherapy and immunotherapy. In this study, we performed a Spearman correlation analysis to assess the association between hub genes and the levels of expression of essential immunological checkpoints such as cytotoxic T-lymphocyte-associated antigen 4, programmed cell death protein 1, and hepatitis A virus cellular receptor 2. (HAVCR2). Our goal was to investigate the role of immune checkpoints in cancer. We analyzed TCGA cancer types and considered significant associations when the P value was less than 0.05. hub genes were significantly correlated with immune checkpoints in all cancer types analyzed. Notably, CCL5 was significantly positively correlated with PD-1 in testicular

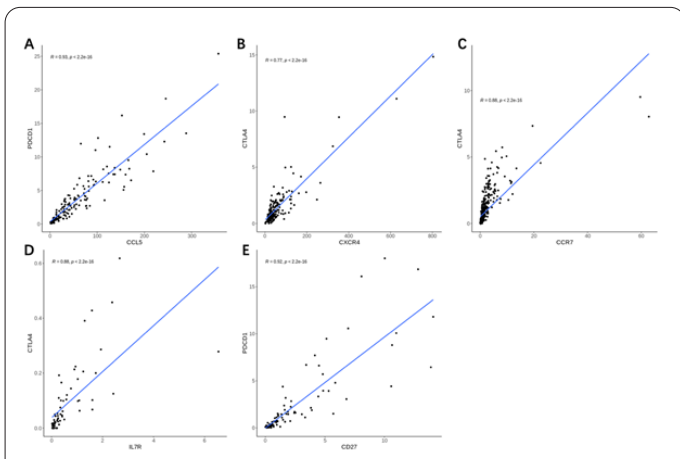


Figure 6. Spearman correlation analysis of immune checkpoint with CCL5, CXCR4, CCR7, IL7R, and CD27. (A) the correlation of CCL5 with PDCD1 in TGCT, (B) the correlation of CXCR4 with CTLA4 in PADD, (C) the correlation of CCR7 with CTLA4 in THCA, (D) the correlation of IL7R with CTLA4 in KICH and (E) the correlation of CD27 with PDCD1 in SKCM. TGCT, testicular germ cell tumors; PADD, pancreatic adenocarcinoma; THCA, thyroid carcinoma; KICH, kidney chromophobe; SKCM, skin cutaneous melanoma.

germ cell tumors (TGCT) (R-value = 0.93, $P < 2.2 \times 10^{-16}$) and CXCR4 was significantly positively correlated with CTLA4 in pancreatic cancer (PADD) (R-value = 0.77, $P < 2.2 \times 10^{-16}$), as shown in Figure 6. In thyroid carcinoma (THCA) (R-value 0.88, $P < 2.2 \times 10^{-16}$), CCR7 was highly positive correlation values with CTLA4 expression levels (KICH) (R-value = 0.88, $P < 2.2 \times 10^{-16}$). Furthermore, there was a significant positive correlation between CD27 and PDCD1 expression levels in skin cutaneous melanoma (SKCM) (R-value = 0.93, $P < 2.2 \times 10^{-16}$).

Gene set enrichment analysis

To understand more about the biological signaling pathways of the hub genes, we ran Gene Set Enrichment Analysis (GSEA) was employed to investigate the likely pathway enrichment of hub gene expression. Figure 7 displays the top three significantly enriched routes. Significant correlations between high levels of CCL5 expression and interferon-gamma response, allograft rejection, and Kras signaling were found using the HALLMARK collection enrichment analysis. Apical junction, allograft rejection, and apoptosis were discovered to be the three main functions of CXCR4, whereas allograft rejection, interferon alpha response, and inflammatory response were revealed to be the three main functions of CCR7. In contrast to CD27, which was discovered to be involved in apical surface, apical junction, and IL2-STAT5 signaling, high levels of IL7R expression were linked to interferon-gamma response, allograft rejection, and angiogenesis. These findings together shed light on the potential functions of the hub genes in the onset and spread of cancer.

Discussion

Cirrhosis-related liver cancer is a complex disease that involves the interplay of various factors, including immune system dysregulation and TME. The liver is a key location of immune cell activity, and immune cells that are resident there, such as Kupffer cells, as well as immune cells that have invaded there, like T cells, play important

roles in the body's response to liver damage. Innate and adaptive immune cells are both activated in the immunological response to liver damage, producing cytokines and chemokines that can increase liver inflammation and fibrosis.

In this work, using gene expression data from liver specimens with and without cirrhosis, immune-related genes were explored for their role in immune initiation and progression of cirrhosis by WGCNA. Using a novel approach, we clustered all 2,441 DEGs obtained by the 'limma' algorithm into 19 modules. Subsequently, we identified the blue module as having the strongest association with LC (cor = 0.57, $P = 6.2 \times 10^{-102}$). Further, the DEGs intersected with the InateDB database to identify immune-related genes. Utilizing the GO enrichment analysis, it was established that the aforementioned genes were predominantly enriched in pathways concerning the activation of T cells and the adhesion of cells. PPI analysis elucidated the interaction between selected genes. There were five genes located in the core, including CCL5, CXCR4, CCR7, IL7R, and CD27, displaying the greatest correlations with other genes selected as immune-related key hub genes for further analysis.

Hematological and solid cancers both exhibit abnormal CCL5 and CCR5 expression and activity (17). Our findings indicate a strong association between CCL5 and CD8⁺T cells as well as PDCD-1. Previous studies have reported that CCL5-deficiency can lead to the upregulation of PDCD-1 and PDCD-L1 expression, reducing resistance to anti-PDCD-1 antibody therapy in a CRC mouse model (18), suggesting a potential therapeutic strategy with checkpoint inhibitors in LC.

CXCR4 is highly expressed in over 23 types of human cancers (19-24). The overexpression of CXCR4 contributes to tumor growth, invasion, angiogenesis, metastasis, relapse, and therapeutic resistance (25-27). Our study found that CXCR4 is closely related to CD4⁺T cells, dendritic cells, macrophages, and B cells, indicating its potential to recruit various immune cells into the tumor and contribute to therapeutic resistance. Additionally, our study demonstrated a correlation between CXCR4 and CTLA-4.

Chemokines, which are tiny heparin-binding proteins,

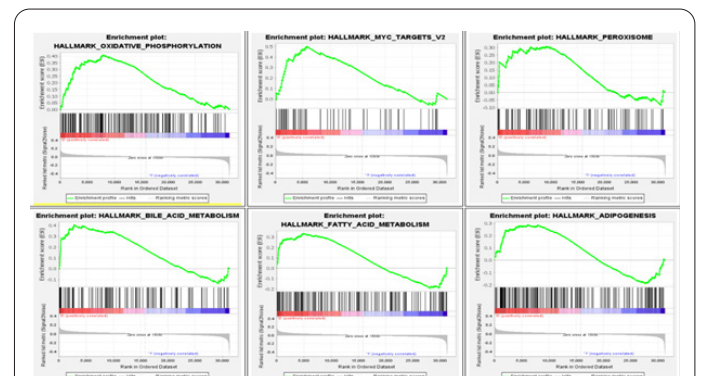


Figure 7. GSEA for clinical samples with low and high hub gene expression. Gene set enrichment is shown to be at the top of the ranked list when the enrichment score (ES) is positive and at the bottom of the list when the ES is negative. The results show that pathways of HALLMARK collection including oxidative phosphorylation, myc target, peroxisome, bile acid metabolism, fatty acid metabolism, and adipogenesis, are enriched in high CCL5, CXCR4, CCR7, IL7R, and CD27 expression groups.

are essential for controlling how cells migrate throughout the body. Based on our investigation, C-C Chemokine Receptor 7 (CCR7) is closely associated with various immune cells, as revealed by the interconnectivity analysis of immune cells and their subsets (28-31). By activating crucial chemokine receptors including CCR5 and CCR7 and boosting sensitivity to chemokines, CTLA-4 can affect T cell motility (32). Also, according to our results, CTLA-4 and CCR7 are highly correlated in LC.

It has been elucidated that IL7R is intricately linked to tumor infiltration within the surrounding environment of lung adenocarcinoma tumors (33). In this research, we hypothesize that IL7R significantly affects the growth of LC via controlling dendritic cell and CD4⁺ T cell infiltration.

CD27 plays a critical role as a costimulatory T-cell receptor in facilitating optimal T-cell priming and memory differentiation. It has potential applications in antitumor therapy by activating cytotoxic CD8⁺ T cells (34). Our study revealed a close association between CD27 and PDCD-1 in LC.

The tumor microenvironment (TME) regulates tumor development and growth through a complex interplay involving immune and non-immune cells, extracellular matrix, and signaling molecules. To explore the potential mechanisms of core genes in disease development, we examined the relationship between key hub genes and immune infiltration. We obtained expression data from TCGA for 33 cancer types, which were used to derive immune cell and immune composite scores through microenvironmental analysis using TIMER, xCell, and ESTIMATE software.

Immune evasion in tumors can be facilitated by dysregulation of immune checkpoints, which act as master regulators within the TME. Immune checkpoint proteins significantly influence cancer immunotherapy and inflammatory responses (35). Inhibition of immune checkpoints can decrease the expression of ligands by cancer cells, reverse the exhaustion state of effector T cells, and enhance anticancer efficacy. Identifying specific immune-related genes and pathways involved in cirrhosis may provide novel therapeutic options for its treatment.

Liver cirrhosis is a multifaceted disease that arises from the interplay of several factors, including dysregulated immune responses, the tumor microenvironment, and immune checkpoint mechanisms. By using weighted gene co-expression network analysis, numerous immune-related genes that contribute to the development and progression of cirrhosis have been identified. Immune checkpoint inhibitors are a treatment option that is currently being researched for this illness. However, additional research is necessary to determine optimal treatment strategies for individuals with cirrhosis-related liver cancer.

Conflict of interests

The authors declared no conflict of interest.

References

1. Tsochatzis EA, Bosch J, Burroughs AK. Liver cirrhosis. *Lancet* 2014; 383(9930): 1749-1761.
2. Gines P, Krag A, Abraldes JG, Sola E, Fabrellas N, Kamath PS. Liver cirrhosis. *Lancet* 2021; 398(10308): 1359-1376.
3. Parola M, Pinzani M. Liver fibrosis: Pathophysiology, pathogenic targets and clinical issues. *Mol Aspects Med* 2019; 65: 37-55.
4. Hernandez-Gea V, Friedman SL. Pathogenesis of liver fibrosis. *Annu Rev Pathol-Mech* 2011; 6: 425-456.
5. Pellicoro A, Ramachandran P, Iredale JP, Fallowfield JA. Liver fibrosis and repair: immune regulation of wound healing in a solid organ. *Nat Rev Immunol* 2014; 14(3): 181-194.
6. Harty MW, Muratore CS, Papa EF, et al. Neutrophil depletion blocks early collagen degradation in repairing cholestatic rat livers. *Am J Pathol* 2010; 176(3): 1271-1281.
7. Boltjes A, van Montfoort N, Biesta PJ, et al. Kupffer cells interact with hepatitis B surface antigen in vivo and in vitro, leading to proinflammatory cytokine production and natural killer cell function. *J Infect Dis* 2015; 211(8): 1268-1278.
8. Krenkel O, Tacke F. Liver macrophages in tissue homeostasis and disease. *Nat Rev Immunol* 2017; 17(5): 306-321.
9. Seki E, Schwabe RF. Hepatic inflammation and fibrosis: functional links and key pathways. *Hepatology* 2015; 61(3): 1066-1079.
10. Langfelder P, Horvath S. WGCNA: an R package for weighted correlation network analysis. *Bmc Bioinformatics* 2008; 9: 559.
11. Niemira M, Collin F, Szalkowska A, et al. Molecular Signature of Subtypes of Non-Small-Cell Lung Cancer by Large-Scale Transcriptional Profiling: Identification of Key Modules and Genes by Weighted Gene Co-Expression Network Analysis (WGCNA). *Cancers* 2019; 12(1):
12. Lin W, Wang Y, Chen Y, Wang Q, Gu Z, Zhu Y. Role of Calcium Signaling Pathway-Related Gene Regulatory Networks in Ischemic Stroke Based on Multiple WGCNA and Single-Cell Analysis. *Oxid Med Cell Longev* 2021; 2021: 8060477.
13. Wang YP, Yu GR, Lee MJ, et al. Lipocalin-2 negatively modulates the epithelial-to-mesenchymal transition in hepatocellular carcinoma through the epidermal growth factor (TGF-beta1)/Lcn2/Twist1 pathway. *Hepatology* 2013; 58(4): 1349-1361.
14. Yoshihara K, Shahmoradgoli M, Martinez E, et al. Inferring tumour purity and stromal and immune cell admixture from expression data. *Nat Commun* 2013; 4: 2612.
15. Aran D, Hu Z, Butte AJ. xCell: digitally portraying the tissue cellular heterogeneity landscape. *Genome Biol* 2017; 18(1): 220.
16. Li T, Fu J, Zeng Z, et al. TIMER2.0 for analysis of tumor-infiltrating immune cells. *Nucleic Acids Res* 2020; 48(W1): W509-W514.
17. Argentova V, Aliev T, Dolgikh D, Pakanova Z, Katrik J, Kirpichnikov M. Features, modulation and analysis of glycosylation patterns of therapeutic recombinant immunoglobulin A. *Biotechnol Genet Eng* 2022; 38(2): 247-269.
18. Zhang S, Zhong M, Wang C, Xu Y, Gao WQ, Zhang Y. CCL5-deficiency enhances intratumoral infiltration of CD8(+) T cells in colorectal cancer. *Cell Death Dis* 2018; 9(7): 766.
19. Balkwill F. The significance of cancer cell expression of the chemokine receptor CXCR4. *Semin Cancer Biol* 2004; 14(3): 171-179.
20. Darash-Yahana M, Pikarsky E, Abramovitch R, et al. Role of high expression levels of CXCR4 in tumor growth, vascularization, and metastasis. *Faseb J* 2004; 18(11): 1240-1242.
21. Vandercappellen J, Van Damme J, Struyf S. The role of CXC chemokines and their receptors in cancer. *Cancer Lett* 2008; 267(2): 226-244.
22. Zlotnik A. New insights on the role of CXCR4 in cancer metastasis. *J Pathol* 2008; 215(3): 211-213.
23. Furusato B, Mohamed A, Uhlen M, Rhim JS. CXCR4 and cancer. *Pathol Int* 2010; 60(7): 497-505.
24. Chatterjee S, Behnam AB, Nimmagadda S. The intricate role of CXCR4 in cancer. *Adv Cancer Res* 2014; 124: 31-82.
25. Orimo A, Gupta PB, Sgroi DC, et al. Stromal fibroblasts present in invasive human breast carcinomas promote tumor growth and angiogenesis through elevated SDF-1/CXCL12 secretion. *Cell*

- 2005; 121(3): 335-348.
26. Eck SM, Cote AL, Winkelman WD, Brinckerhoff CE. CXCR4 and matrix metalloproteinase-1 are elevated in breast carcinoma-associated fibroblasts and in normal mammary fibroblasts exposed to factors secreted by breast cancer cells. *Mol Cancer Res* 2009; 7(7): 1033-1044.
 27. Kojima Y, Acar A, Eaton EN, et al. Autocrine TGF-beta and stromal cell-derived factor-1 (SDF-1) signaling drives the evolution of tumor-promoting mammary stromal myofibroblasts. *P Natl Acad Sci Usa* 2010; 107(46): 20009-20014.
 28. Campbell JJ, Murphy KE, Kunkel EJ, et al. CCR7 expression and memory T cell diversity in humans. *J Immunol* 2001; 166(2): 877-884.
 29. Sanchez-Sanchez N, Riol-Blanco L, de la Rosa G, et al. Chemokine receptor CCR7 induces intracellular signaling that inhibits apoptosis of mature dendritic cells. *Blood* 2004; 104(3): 619-625.
 30. Schneider MA, Meingassner JG, Lipp M, Moore HD, Rot A. CCR7 is required for the in vivo function of CD4+ CD25+ regulatory T cells. *J Exp Med* 2007; 204(4): 735-745.
 31. Pereira JP, Kelly LM, Cyster JG. Finding the right niche: B-cell migration in the early phases of T-dependent antibody responses. *Int Immunol* 2010; 22(6): 413-419.
 32. Brunner-Weinzierl MC, Rudd CE. CTLA-4 and PD-1 Control of T-Cell Motility and Migration: Implications for Tumor Immunotherapy. *Front Immunol* 2018; 9: 2737.
 33. Wang X, Chang S, Wang T, et al. IL7R Is Correlated With Immune Cell Infiltration in the Tumor Microenvironment of Lung Adenocarcinoma. *Front Pharmacol* 2022; 13: 857289.
 34. Hasan S, Awasthi P, Malik S, Dwivedi M. Immunotherapeutic strategies to induce inflection in the immune response: therapy for cancer and COVID-19. *Biotechnol Genet Eng* 2022: 1-40.
 35. Dyck L, Mills K. Immune checkpoints and their inhibition in cancer and infectious diseases. *Eur J Immunol* 2017; 47(5): 765-779.